

# Comparing the characteristics of surface-passivated and electropolished 316L stainless steel

Patrick Lowery, *Unit Instruments*; and Daryl Roll, *Astro Pak*

Because of the large number of corrosive and reactive gases used in semiconductor device manufacturing, superior corrosion resistance and moisture dry-down performance are critical parameters of the gas distribution systems used in IC fabs. Take, for example, the case of corrosion while under halogen gas service. In the presence of molecular moisture, halogen gases such as hydrogen chloride and boron chloride can hydrolyze (ionize) to form their respective acids and react with the metal surface. The resultant product of these reactions is halide particles, which can degrade the cleanliness of the distribution system and contribute to microcontamination on the silicon wafer surface.<sup>1</sup> Although this type of reaction is the most common, it is just one type of corrosion mechanism that can occur in semiconductor gas systems.

The most widely specified material for gas distribution applications, AISI 316L stainless steel has an intrinsic corrosion resistance because of its ability to form a protective oxide or "passive" layer on its surface by alloying >12% chromium with iron, nickel, and molybdenum. This protective layer is thought to consist of a heterogeneous chromium oxide film ( $\text{Cr}_2\text{O}_3$ ) along with elemental iron, nickel, and their respective oxides. The exact nature of the chemical properties, atomic structure, and formation mechanism of this film are as yet undetermined. In general, this passive layer protects the steel from oxidation. However, when subjected to extremely corrosive environments (for example, halide gases in the presence of moisture), the heterogeneous film is attacked and chemical reduction occurs. When the oxide film layer is destroyed beyond regeneration, localized corrosion takes place in the bulk alloy and reaction by-products are generated in the form of halide particulates.<sup>2,3</sup>

The corrosion resistance at the steel's surface can be enhanced by increasing the amount of chromium that can form  $\text{Cr}_2\text{O}_3$  in the presence of an oxidizing environment. This is achieved by removing iron, iron oxides, and other residual metals from the upper 20 to 50 Å of the material, where they present oxidizable elements that can become possible corrosion sites. The depth of the chromium enrichment layer will determine the extent of selective chemical reduction that can take place before localized corrosion becomes prominent.<sup>4</sup> There are a variety of surface passivation procedures that can achieve the desired chromium enrichment in 316L stainless steel; however, the study reported in this article focused on the comparative effectiveness of electropolishing and organic acid/chelate passivation. The elemental composition and moisture desorption characteristics of surfaces treated with these techniques were compared using several evaluation methods to determine whether the more environmentally friendly organic acid/chelate process could meet the requirements of the semiconductor industry.

## Passivation Procedures

The electropolishing process uses an electrolytic cell to remove metal from a workpiece. The workpiece is immersed in a specially formulated electrolyte solution of blended mineral acids and acts as the anode in the electrochemical cell. A cathode is then immersed in the electrolyte solution to complete the electrical circuit and a dc current is applied. Such factors as the applied electrical current, workpiece geometry and surface finish, and electrolyte chemistry determine the rate at which material is removed from the workpiece surface. In the case of stainless-steel alloys such as 316L, iron and nickel atoms are more easily extracted from the crystal lattice than are chromium atoms. That is, iron and nickel are attacked preferentially during the electrolytic process, leaving behind an enhanced surface layer of chromium, which then forms the passive enrichment layer.<sup>5</sup> This process also tends to smooth the surface finish since the metals are removed from surface peaks or high points.

The alternative passivation process evaluated in this study involves the use of organic citric acid in conjunction with specially formulated chelant systems containing ethylenediaminetetraacetic acid (EDTA, commonly used as a food preservative), reducing agents, buffers, and surfactants. (A *chelant* is a reactive molecule that can bond with metal ions and effectively render them inert.<sup>6</sup>) In the case of 316L stainless steel, the acid/chelant system selectively dissolves and chelates metallic inclusions, iron, and nickel, leaving the free chromium/chromium oxide behind. Since the chelant-metal complexes are rendered chemically inert after the dissolved metallic ions become attached, they can subsequently be swept from the surface without precipitation or redeposition elsewhere.<sup>7</sup> The surface must be mechanically polished or lapped prior to passivation to provide the required surface smoothness. The acid/chelant process will not affect the surface finish.

Because of the nature of the chemicals used, the organic acid/chelant treatment raises relatively few safety and environmental concerns. When citric acid is specially blended with DI water and different chelant systems, the pH level of the solution is between 2 and 12; thus, the chemicals do not meet the criteria of *hazardous waste* and can be disposed of via a sewer system with the proper permitting. In contrast, the nitric acid commonly used after electropolishing processes requires special disposal procedures and has long-term liabilities associated with it. In addition, because the acid/chelant treatment is not electrochemical in nature, it does not require power and specially designed electrodes.

## Experimental Procedures

**Sample Preparation.** The stainless steel used in this study was VIM/VAR 316L (Carpenter Technology, Reading, PA), which had an ASTM grain size number of 5. Table I shows the elemental composition of the particular lot that was used. The steel was machined into flat 1½-in.-diam sections for compatibility with the testing apparatuses; all sample pieces were ground flat and then precision lapped. After some samples were passivated using the organic acid/chelant system (Ultra Pass; Astro Pak, San Diego) and others were electropolished using a standard acid-based electrolyte process, all of the treated pieces were bagged in a Class 100 environment to avoid contaminating the surfaces with atmospheric hydrocarbons or particulates.

Element (wt%)										
Cr	Ni	Mo	P	S	C	Mn	Cu	Si	Ca	Al
16.76	12.99	2.22	0.011	0.003	0.017	1.25	0.03	0.54	0.01	0.003

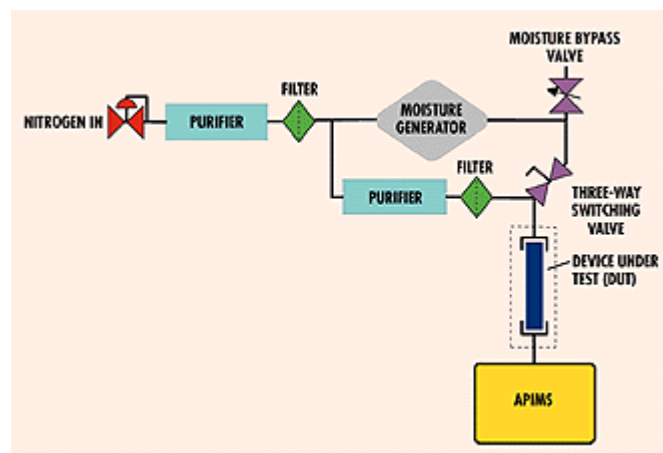
*Table I: Elemental analysis of test samples machined from VIM/VAR 316L stainless steel.*

**ESCA Evaluation.** The treated samples were first analyzed using electron spectroscopy for chemical analysis (ESCA; also commonly referred to as x-ray photoelectron spectroscopy). During this procedure, the sample surface is bombarded with monochromatic x-rays (in this case, Al K\*), which allows electrons within the bulk material's atomic structure to escape from their inner electron orbital shells. The energy spectra are reported in terms of binding energy versus intensity. With the use of sensitivity factors, peak intensities provide quantitative data on the elemental composition of the sample surface. The oxidation states of these elemental species are also determined.<sup>8,9</sup>

**AES Analysis.** Auger electron spectrometry (AES) was performed to gather additional data on the elemental composition of the steel surface, down to a depth of ~150 Å. Instead of using x-rays to excite electrons within the sample (as in ESCA), AES uses a finely focused electron beam as the incident radiation. An ion-sputtering (etch) process enables the sample's elemental concentration to be plotted as a function of depth. Sputtering and AES analysis are alternated until the desired depth is reached. The depth measurement is obtained by calibrating the ion-sputtering process with a thermally grown silicon oxide (SiO<sub>2</sub>) or electrolytically grown tantalum oxide (Ta<sub>2</sub>O<sub>5</sub>) standard. (A calibration standard must be used in order to compare materials of similar composition.) In this study, the depth profile was obtained by observing the Auger peaks for carbon, chromium, nickel, iron, and oxygen after the sample had been etched with an argon ion beam at 5–10-Å intervals.<sup>10–12</sup> Although this type of analysis can be useful for obtaining information regarding the elemental composition below the top surface of a sample, its accuracy is limited as a result of the sensitivity factors, calibration standards, and data interpretation used. ESCA is considered much more accurate for quantitative calculations.

**APIMS Analysis.** Atmospheric pressure ionization mass spectrometry (APIMS) is a form of mass analysis that allows one to measure extremely low (parts-per-trillion level) concentrations of impurities in a gas stream. The sample gas is partially ionized by an atmospheric pressure corona discharge. The energy of this process results in extremely high collision densities, which in turn result in ionization of nearly 100% of all gaseous impurities. The fact that these impurities have lower ionization energies than the carrier gas contributes to the extremely high sensitivity of the technique. This method also offers very high time resolution, which, coupled with its high sensitivity, make it the only analytical technique capable of quantifying the desorption of moisture from the Cr<sub>2</sub>O<sub>3</sub> passive layer on stainless steel.<sup>13</sup>

During this study, the APIMS analyses were performed by flowing purified nitrogen (N<sub>2</sub>) through the test pieces at a rate of 1.2 L/min. A moisture generator with a bypass metering valve was used to expose the samples to a 200-ppb-moisture challenge gas. Figure 1 shows the testing system schematically. The incoming N<sub>2</sub> was filtered (0.01 μm) and purified to a moisture level of <1 ppb at the source, and a second getter immediately adjacent to the all-metal, three-way valve switched between the challenge gas and control gas was used to ensure that the background impurity concentration of the control was below the detection level of the spectrometer. The device under test was contained in an insulated and temperature-controlled column, and wetted surface areas downstream of the sample were minimized.



that

Figure 1: Schematic of the APIMS test apparatus

Bypass N<sub>2</sub> was supplied to the APIMS while each sample piece was installed and allowed to dry down to the specified background level. The switching valve was then actuated and left open for 20 minutes, permitting the sample to equilibrate at a 200-ppb moisture level. After the moisture exposure interval, the valve was closed, control gas was allowed to flow through the apparatus, and moisture concentration was monitored until it fell to the original background level. The rate of moisture desorption from the sample surface thus obtained provides an insight to the quality of the passive layer at the steel surface.

**Surface Roughness Tests.** In addition to the analytical techniques described above, scanning electron microscopy (SEM) and contact surface profilometry were used to measure the samples' surface roughness.

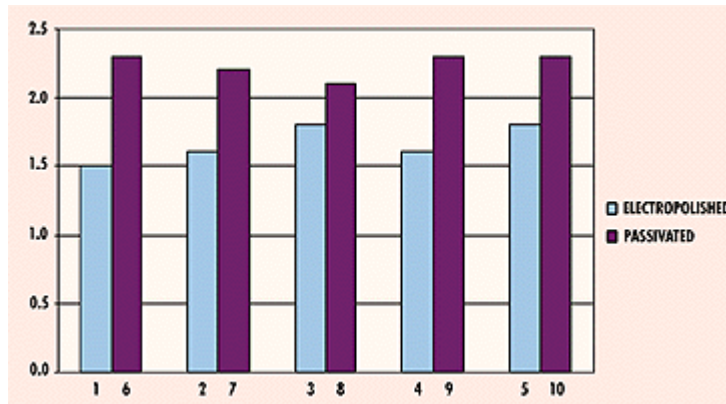


Figure 2: Elemental chromium-to-iron ratios for both electropolished and passivated samples (numbers 1–5 and 6–10, respectively).

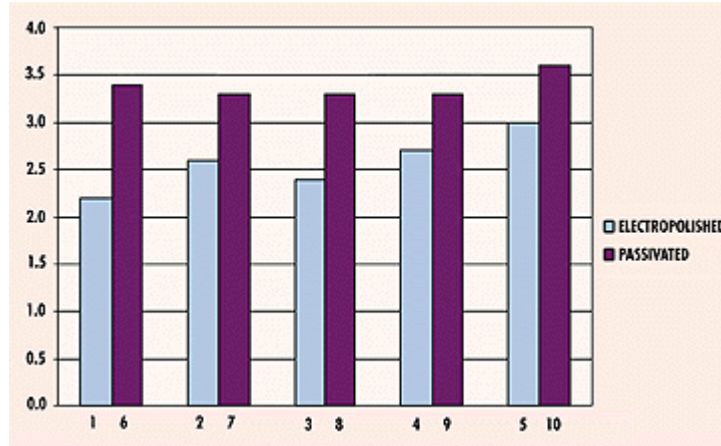


Figure 3: CrO<sub>x</sub>/FeO<sub>x</sub> ratios for both electropolished and passivated samples (numbers 1–5 and 6–10, respectively).

## Results and Discussion

**ESCA Results.** The ESCA analyses provided data on the elemental and oxide surface chemistries of the treated samples. Figure 2 compares the chromium-to-iron (Cr/Fe) ratios for five surfaces modified by the electropolishing process (samples 1—5) with those of five samples modified by organic acid/chelate passivation (samples 6—10), while Figure 3 compares the  $\text{CrO}_x/\text{FeO}_x$  ratios for the same samples. As the figures show, the Cr/Fe and  $\text{CrO}_x/\text{FeO}_x$  ratios for the passivated samples were higher than the values obtained for the electropolished samples, and the passivated samples' Cr/Fe ratios exceeded the 1.5:1 commonly accepted by the semiconductor industry for ultra-high-purity gas distribution systems. Specifically, the average Cr/Fe ratio for the passivated samples was 2.2:1 versus 1.7:1 for the electropolished samples; the average  $\text{CrO}_x/\text{FeO}_x$  ratio for the passivated samples was 3.4:1 versus 2.5:1 for the electropolished samples. The higher surface chromium and chromium oxide levels on the passivated samples will contribute to a higher surface corrosion resistance than that of the electropolished samples because the removal of surface iron and metallic contaminants reduces the potential for reactive-site corrosion. (It should be mentioned that the surface chemistries obtained from the electropolishing process used in this analysis are not indicative of all such processes; better results should be possible by varying such parameters as electrolyte chemistry and specialized electrode geometry.)

Sample No.	P	S	Cl	C	N	O	Cr	Fe	Ni	Si	Na	Ca
2	0.1	0.0	0.1	29.1	0.1	39.4	14.3	12.0	4.6	0.4	0.0	0.0
3	0.8	0.3	0.0	30.4	0.9	35.5	12.8	10.5	5.0	0.1	1.9	1.9
5	0.1	0.0	0.0	33.8	0.8	37.5	11.9	11.0	4.7	0.2	0.0	0.0

*Table II:*

*Surface elemental compositions of selected electropolished samples.*

Sample No.	P	S	Cl	C	N	O	Cr	Fe	Ni	Si	Na	Ca
7	0.3	1.0	0.0	50.0	1.8	28.2	5.9	9.6	3.0	0.2	0.0	0.0
8	0.0	1.8	0.1	44.5	2.7	30.1	7.1	10.4	3.2	0.2	0.0	0.0
9	0.1	0.1	0.2	41.5	0.9	30.1	10.9	11.4	4.7	0.1	0.0	0.0

*Table III: Surface elemental composition of selected passivated samples.*

**AES Results.** The AES results revealed information about the compositional profile below the sample surface as well as the elemental composition at the surface. Tables II and III present surface elemental composition data estimated from the AES survey spectra for the sample numbers listed. As shown, the elemental composition of the two types of samples did not vary significantly except for the chromium content, which was higher for the passivated samples than the electropolished samples. The phosphorus, chlorine, sodium, calcium, and, to some extent, carbon concentrations can be traced to impurities introduced during material handling and analysis. As mentioned earlier, it should be remembered that

ESCA is a much more exact way to quantify the impurity concentrations at the surface than AES is. Although not shown in these tables, the passivation process is known to remove earth metal contaminants (aluminum and magnesium, for example) that can form pitting sites, and base metal contaminants (manganese, sulfur, phosphorus, and carbon) that form sulfides and carbides.

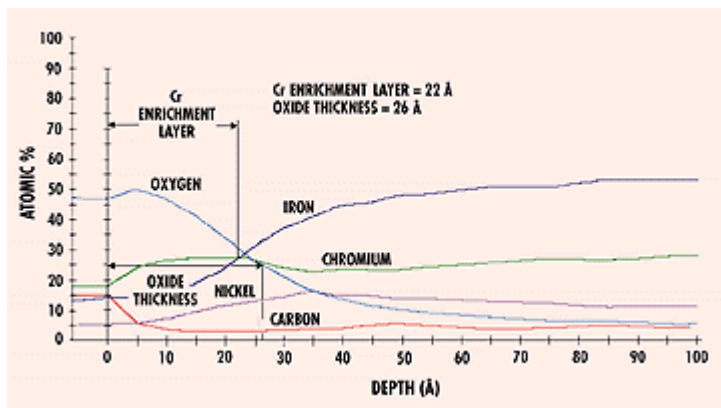


Figure 4: AES depth profile for sample number 2.

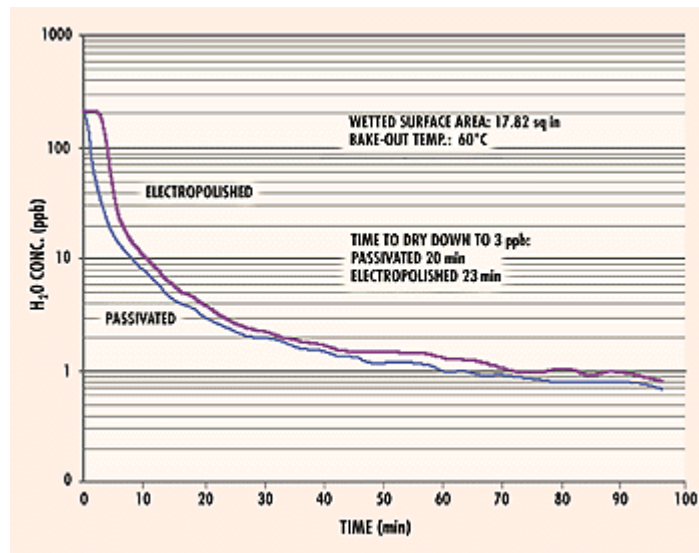
Figure 4 shows an AES compositional depth profile for sample number 2. The atomic percentages of oxygen, chromium, iron, nickel, and carbon are plotted as a function of distance from the surface, and the oxide thickness and chromium enrichment layer are also indicated. The chromium oxide thickness is defined as the depth at which the oxygen signal has fallen to half of its maximum peak height (the full-width, half-maximum, or FWHM technique). The depth of the chromium enrichment layer is the value at which the chromium concentration intersects the iron concentration. The depth of the carbon layer or the thickness of surface organics also can be determined using an FWHM technique.

Table IV: Results from AES depth profiles performed on passivated and electropolished samples (all depths are expressed in SiO<sub>2</sub> equivalents).

Sample Type	Oxide Thickness (Å)	Max. Depth of Enrichment (Å)	Depth of Cr Enrichment (Å)	Iron Oxide Layer (Å)	Carbon Layer (Å)
<b>Passivated:</b>	31.0	23.0	23.0	0.0	5.0
	26.0	22.0	22.0	0.0	4.0
	37.0	27.0	27.0	0.0	10.0
	31.0	24.0	24.0	0.0	8.0
	31.0	24.0	24.0	0.0	4.0
	34.0	23.0	23.0	0.0	10.0
<b>Average</b>	<b>31.7</b>	<b>23.8</b>	<b>23.8</b>	<b>0.0</b>	<b>6.8</b>
<b>Electropolished:</b>	30.0	23.0	23.0	0.0	20.0
	30.0	25.0	25.0	0.0	6.0
	29.0	25.0	23.0	2.0	6.0
	29.0	25.0	25.0	0.0	9.0
	22.0	20.0	20.0	0.0	6.0
	21.0	18.0	18.0	0.0	6.0
<b>Average</b>	<b>26.8</b>	<b>22.7</b>	<b>22.3</b>	<b>0.3</b>	<b>8.8</b>

Table IV summarizes the AES depth profile results for both the passivated and electropolished samples. The average oxide thickness and chromium enrichment layers were 31.7 and 23.8 Å, respectively, for the passivated samples, and 26.8 and 22.3 Å, respectively, for the electropolished samples. These data indicate that the passivation process results in thicker chromium enrichment and oxide layers with no observable iron oxide at the surface. Both the iron oxide and carbon layers were lower for passivated samples when compared to electropolished samples, which may or may not be attributable to parameters associated with the electropolishing process. It is possible that the post process handling of the electropolished samples was not as well controlled as for the passivated samples. However, it is clear that the passivation process provides chromium enrichment depths and subsequent Cr<sub>2</sub>O<sub>3</sub> passive layers that exceed those achieved by electropolishing. In addition, all of the oxide depths obtained for the passivated samples exceed the 25-Å minimum that is commonly accepted for UHP gas distribution systems.

**APIMS Results.** The moisture desorption characteristics of a gas distribution system indirectly indicate the quality of the passivation layer and surface finish of its stainless-steel components. Because moisture is the most difficult impurity to remove from UHP gas systems, the passivation layer's moisture desorption characteristics are of paramount importance.



*Figure 5: Moisture desorption curves for both electropolished and passivated samples.*

Figure 5 shows moisture desorption curves for both passivated and electropolished samples, which had been allowed to dry down to 3-ppb moisture levels before the 200-ppb moisture challenge was introduced. Both types of samples had surface finishes of 5 µin. Ra. The data show that the passivated samples took less time than the electropolished samples (20 minutes versus 23 minutes) to desorb to a concentration of 3 ppb following the challenge. Both of the dry-down curves, however, show regions dominated by two different desorption mechanisms: physisorption and chemisorption. The initial fairly steep slopes correspond to the physisorption of moisture from other layers of adsorbed moisture. The lesser slopes correspond to chemisorption of moisture from the surface or from the passivation layer of the stainless steel. The difference in chemisorption rates between the passivated and electropolished samples can be attributed to several factors, including the different surface roughness and surface chemistry (i.e., CrO<sub>x</sub>/FeO<sub>x</sub> and Cr/Fe ratios) of the samples. Because of the lack of significant data pertaining to the exact adsorption mechanisms of H<sub>2</sub>O on heterogeneous oxides (as opposed to single-crystal oxides), the desorption curves show only qualitative characteristics of the passivation layers.

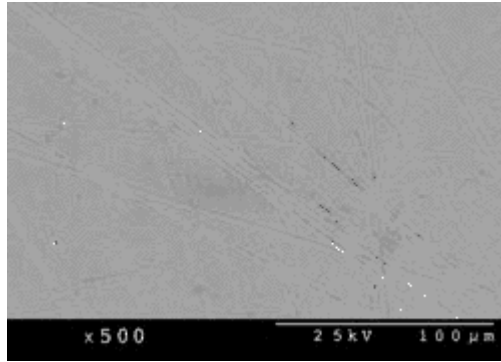


Figure 6: SEM micrograph of a lapped and passivated surface.

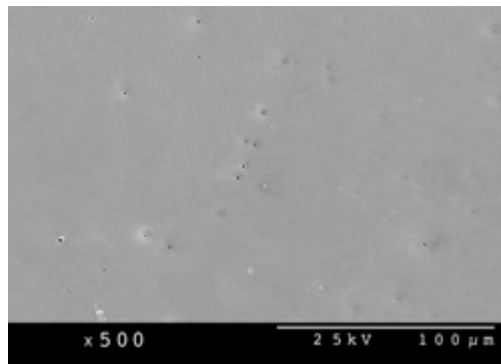


Figure 7: SEM micrograph of a lapped and electropolished surface.

**Surface Roughness Results.** Electropolishing is used not only to modify surface chemistries but to achieve smoother surface finishes. Figures 6 and 7 show SEM micrographs of a lapped and passivated sample and a lapped and electropolished sample, respectively. The electropolished surface appears to be quite smooth with the exception of oxide or sulfide inclusions (black spots). In contrast, the passivated surface exhibits the types of striations or scratches caused by the surface abrasion that occurs during the lapping process.

Sample Type	Ra ( $\mu\text{in.}$ )	rms ( $\mu\text{in.}$ )
Lapped	0.984	1.378
Lapped and passivated	1.181	1.575
Lapped and electropolished	5.906	7.874

Table V: Surface profilometry results for a control sample and the samples depicted in Figures 6 and 7.

Table V shows contact surface profilometry data from the same two samples. These data reveal that the electropolished sample actually had a greater surface roughness than the passivated sample. When measured after electropolishing, the surface roughness of the sample had increased from approximately 1  $\mu\text{in. Ra}$  to approximately 6  $\mu\text{in. Ra}$ . As a result of the higher internal (lattice) energy associated with defects, the electropolishing process preferentially attacks areas that have inclusions or abnormalities. This preferential attack results in an overall rougher surface even though it appears smooth at high magnifications. **The passivation procedure does not alter the surface topography while enriching the chromium concentration at the surface.**

## Conclusion

In a study comparing the effectiveness of organic acid/chelant passivation and electropolishing for producing a corrosion-resistant passive layer on the surface of 316L stainless steel, the passivation procedure produced higher chromium-to-iron ratios, chromium oxide/iron oxide ratios, and oxide thickness when measured with ESCA and AES. When the moisture desorption response to a 200-ppb challenge was quantified using APIMS, the passivated samples showed markedly faster desorption times than the electropolished samples.

The passivation process uses organic citric acid and specially formulated chelant systems. These substances typically do not require special containment, storage, or disposal procedures, unlike the strong mineral acids used in electropolishing. In addition, because the passivation process is not electrochemical in nature, it does not require specialized electrode configurations that are particular to the workpiece geometry. In conclusion, the passivation process studied met semiconductor industry specifications and can provide a viable and environmentally "green" alternative to electropolishing for UHP gas distribution systems.

## Acknowledgments

The authors would like to thank Surface Science Laboratories for performing comprehensive and detailed compositional analyses and Jeffrey Briesacher at SAES Pure Gas for the use of his laboratory and expertise in the APIMS analysis.

## References

1. Ohmi T, Nakagawa Y, Masakazu N, et al., "Formation of Chromium Oxide on 316L Austenitic Stainless Steel," *Journal of Vacuum Science Technology*, A14(4):2505—2509, 1996.
2. Barbosa MA, "The Pitting Resistance of AISI 316 Stainless Steel Passivated in Diluted Nitric Acid," *Corrosion Science*, 23(12):1303—1305, 1983.
3. Walls MG, Ponthieux A, Rondot B, and Owen RA, "In Situ Observation of the Oxidation and Reduction Processes on Fe-Cr Alloys," *Journal of Vacuum Science Technology*, A14(3):1362, 1996.
4. Askeland D, *The Science and Engineering of Materials*, Boston, PWS Publishers, pp 507—509, 1985.
5. Menon GR, "Rough and Its Removal from High-Purity Water Systems," *BioPharm*, 7(June):40—43, 1990.
6. Zumdahl SS, *Chemistry*, Lexington, MA, DC Heath, pp 840—841, 1986.
7. Roll D, "Current Methodologies and Chemistries Utilized in Effective Passivation Procedures," in *Proceedings of Interphex 96*, Norwalk, CT, Reed Exhibition Cos., pp 134—141, 1996.
8. Powell CJ, in *Quantitative Surface Analysis of Materials*, McIntyre NS (ed), Philadelphia, ASTM, p 5, 1978.
9. Joshi A, Davis LE, and Palmberg PW, in *Methods of Surface Analysis*, Czanterna AW (ed), Amsterdam, Elsevier, p 218, 1975.
10. Briggs D, and Seah M (eds), *Practical Surface Analysis: Auger and X-ray Photoelectron Spectroscopy*, 2nd ed, New York, Wiley, pp 186—192, 1990.
11. *SEMASPEC Test Method for Auger Electron Spectroscopy (AES) Analysis of Surface and Oxide Composition of Electropolished Stainless Steel Tubing for Gas Distribution Systems*, Sematech Technology Transfer #91060573B-STD, Austin, TX, Sematech, pp 1—5, 1993.
12. Ohmi T, and Nitta T, *Ultra Pure Gas Delivery System*, Institute of Basic Semiconductor Technology Development, Tokyo, Realize, pp 401—429, 1986.
13. Henrich VE, and Cox PA, *The Surface Science of Metal Oxides*, Cambridge, UK, Cambridge University Press, pp 255—269, 352—353, 1994.

**Patrick Lowery** is principal quality engineer for the Z-Bloc modular gas systems division of Unit Instruments (Yorba Linda, CA). Previously, he was analytical services manager at Control Systems, which is now part of Unit Instruments. Lowery serves on the SEMI task forces for modular gas systems, surface passivation, and stainless steel. He graduated with honors from the New Mexico Institute of Mining and Technology with a BS in materials engineering, and while serving as a research and teaching assistant at the institute, conducted laboratory and classroom lectures for physical and mechanical metallurgy and transmission electron microscopy courses. (Lowery can be reached at 714/921-2640.)

**Daryl Roll** is vice president of Astro Pak (San Diego), a provider of precision cleaning and passivation services to industries that use stainless-steel equipment with ultrapure surface requirements. He manages western U.S. operations and production as well as directing the corporate research effort in semiconductor and high-purity processing. Roll has more than 20 years' experience in chemical processing, including the design of process pipe cleaning equipment, chemical process technology, and precision cleaning of ultra-high-purity systems. His expertise also extends to field engineering, chemicals and metals testing, and research and project management. He holds a BS in chemistry and earth science from California State University, Fullerton.

---